Journal of Power Sources 341 (2017) 387–395

Contents lists available at ScienceDirect

Journal of Power Sources

journal homepage: www.elsevier.com/locate/jpowsour

Short communication

Modified electrochemical parameter estimation of NCR18650BD battery using implicit finite volume method

T.R. Ashwin, A. McGordon, W.D. Widanage, P.A. Jennings*

WMG, University of Warwick, Coventry, CV4 7AL, UK

HIGHLIGHTS

- Method to parametrise P2D electrochemical model for any cell chemistry.
- Numerical expression to calculate OCV+ from the discharge voltage.
- Butler-Volmer equation is modified to a quadratic equation improving the efficiency.
- The model results improve on the accuracy reported in the previous literature.

ARTICLE INFO

Article history:
Received 22 July 2016
Received in revised form
22 September 2016
Accepted 5 December 2016

Keywords:
Lithium-ion battery
Electrochemical model
Pseudo two dimensional model
Parameter estimation

ABSTRACT

The Pseudo Two Dimensional (P2D) porous electrode model is less preferred for real time calculations due to the high computational expense and complexity in obtaining the wide range of electro-chemical parameters despite of its superior accuracy. This paper presents a finite volume based method for re-parametrising the P2D model for any cell chemistry with uncertainty in determining precise electro-chemical parameters. The re-parametrisation is achieved by solving a quadratic form of the Butler-Volmer equation and modifying the anode open circuit voltage based on experimental values. Thus the only experimental result, needed to re-parametrise the cell, reduces to the measurement of discharge voltage for any C-rate. The proposed method is validated against the 1C discharge data and an actual drive cycle of a NCR18650BD battery with NCA chemistry when driving in an urban environment with frequent accelerations and regenerative braking events. The error limit of the present model is compared with the electro-chemical prediction of Li_yCoO_2 battery and found to be superior to the accuracy of the model presented in the literature.

1. Introduction

Electro-chemical characteristics, and the physical processes inside a lithium-ion battery can be captured by solving the governing equations over a porous layout, first proposed by Doyle et al. [1] and the model is widely known as Pseudo Two Dimensional (P2D) model.

Ageing models available in the literature assume a continuous solvent reduction reaction for the capacity fade. More details can be found in Ramadass et al. [2]. Many studies proved that ageing of the cell is strongly coupled with temperature which accelerates the Solid Electrolyte Interphase (SEI) layer growth [3]. Hence it is important to solve the full energy equation to capture the thermal effects by solving an accurate distributed thermal model [4,5]. Very few studies have looked into the coupled thermal and ageing studies, for example by Xie et al. [6], Tanim and Rahn [7] and Ashwin et al. [8].

Inclusion of the above these effects have significantly increased the computational cost which makes P2D unsuitable for real-time prediction. More details can be found in Wang et al. [9], Subramani et al. [10], Haran et al. [11] and a comparative study in Santhanagopalan et al. [12]. The temperature variation can be captured by a lumped parameter model [13,14].

Most of the above mentioned models focus on simplifying the chemical process inside a battery by using linear equations which makes the model less accurate in predicting the chemical kinetics. Some studies have looked into reducing the computational

* Corresponding author.
E-mail addresses: A.T.Rajan@warwick.ac.uk (T.R. Ashwin), Paul.Jennings@warwick.ac.uk (P.A. Jennings).

http://dx.doi.org/10.1016/j.jpowsour.2016.12.023

requirements by improving the numerical schemes of a P2D model for example Dao et al. [15] and Lee et al. [16]. The re-parametrisation of a pseudo two dimensional model requires information about an extensive number of physical parameters, for example, porosity, particle size, solid and electrolyte conductivity and the diffusion coefficients. A parameter estimation using a non-linear least squares regression technique is proposed by Santhanagopalan et al. [17].

This paper focuses on improving two main complementary aspects of modelling which need further attention; computational method and re-parametrisation. The computational requirement of a P2D model can be drastically reduced by adopting the implicit formulation presented in this paper. The re-parametrisation helps the modellers to switch between different cell chemistries thereby minimising the extensive measurements of aforementioned physical parameters or in the cases where there is an uncertainty in electrochemical parameters. The finite volume methodology can be used as a tool to simplify the governing equations and to calculate the positive open circuit voltage of the battery by solving a quadratic form of Butler-Volmer equation. The modification of positive Open Circuit Voltage (OCV) had been suggested as a possible solution to parametrise an electrochemical model by several researchers but was never adapted due to the difficulty in implementation [17]. This proposed method is applied to parametrise a NCR18650BD using known electrochemical values from SONY 18650 Li_yCoO_2 chemistry. The model predictions are validated against the complete drive cycle and 1C discharge voltage. The ageing parameters can be also handled by the an iterative procedure described in the paper.

2. Model development & governing equations

The governing equations are discretised over the finite volume-finite difference mesh layout as shown in Fig. 1.

2.1. Li^+ ions in electrolyte phase

Conservation of Li in electrolyte phase can be represented in a finite volume-finite difference [18,19] frame work as:

$$\underbrace{\frac{\partial}{\partial t}(\varepsilon_e c_e)}_{\text{Time dependent term}} = \underbrace{\nabla\cdot\left(D_{e,eff}\nabla c_e\right)}_{\text{Diffusion term}} + \underbrace{\frac{1-t^+}{F}(J_s+J_1)}_{\text{Source term}} \tag{1}$$

The boundary condition at the current collector interface:

$$\left.\frac{\partial c_e}{\partial x}\right|_{x=0} = 0,\ \left.\frac{\partial c_e}{\partial x}\right|_{x=L} = 0$$

The time dependent term descretization is given by:

$$\frac{\partial}{\partial t}(\varepsilon_e c_e) = \frac{(\varepsilon_e c_e)|_t - (\varepsilon_e c_e)|_{t-\Delta t}}{\Delta t}$$

The diffusion term descretization is given by:

$$\nabla\cdot\left(D_{e,eff}\nabla c_e\right) = \frac{\left(D_{e,eff}\nabla c_e\right)|_{x+\Delta x} - \left(D_{e,eff}\nabla c_e\right)|_x}{\Delta x}$$

The diffusion term contribution at the first volume near the negative electrode current collector interface only carries contribution from the east face flux due to the zero gradient boundary condition.

2.2. Li^+ ions in the solid phase

$$\frac{\partial}{\partial t}c_s = \frac{D_s}{r^2}\frac{\partial}{\partial r}\left(r^2\frac{\partial}{\partial r}c_s\right) \tag{2}$$

2.3. Electrolyte phase potential

$$\nabla\cdot\left(\kappa^{eff}\nabla\phi_e\right) + \nabla\cdot\left(\kappa_D^{eff}\nabla In(c_e)\right) + J_1 + J_s = 0 \tag{3}$$

The above equation reduces to Poisson's equation of the following form:

$$L\frac{\partial^2\phi_e}{\partial^2 x} = K$$

where L and K are constants. Thus the solution of this Poisson's equation can take different values with an added constant $\phi_e + Q$. The boundary condition at the negative electrode can be applied as given below:

$$\left.\frac{\partial\phi_e}{\partial x}\right|_{x=0} = 0$$

In this formulation, the electrolyte potential at the first nodal point is taken as zero. Thus the second nodal point potential is also zero due the Neumann boundary condition applied at the negative electrode-current collector interface.

2.4. Solid phase potential

$$\nabla\cdot\left(\sigma_{eff}\nabla\phi_s\right) = (J_1 + J_s) \tag{4}$$

Thus the above equation is a Poisson's equation of the form:

$$L\frac{\partial^2\phi_s}{\partial^2 x} = K$$

The solution of the Poisson's equation is of the form $\phi_s + Q$. The actual value of the constant (i.e. value of Q) can be found by solving the quadratic form of the Butler-Volmer equation (Equation (5)). Equation (6) gives the value to correct the negative profile and Equation (7) gives the value to correct the positive profile.

The boundary condition for Equation (2), Equation (3) and Equation (4) can be found in Ashwin et al. [8].

2.5. Intercalation reaction

The Butler-Volmer equation:

$$J_1 = a_s i_o\left\{\exp\left(\frac{\alpha_{n,p}F\eta}{RT}\right) - \exp\left(-\frac{\alpha_{n,p}F\eta}{RT}\right)\right\} \tag{5}$$

In the above equation let

$$\theta = \exp\left(\frac{\alpha F\eta}{RT}\right)$$

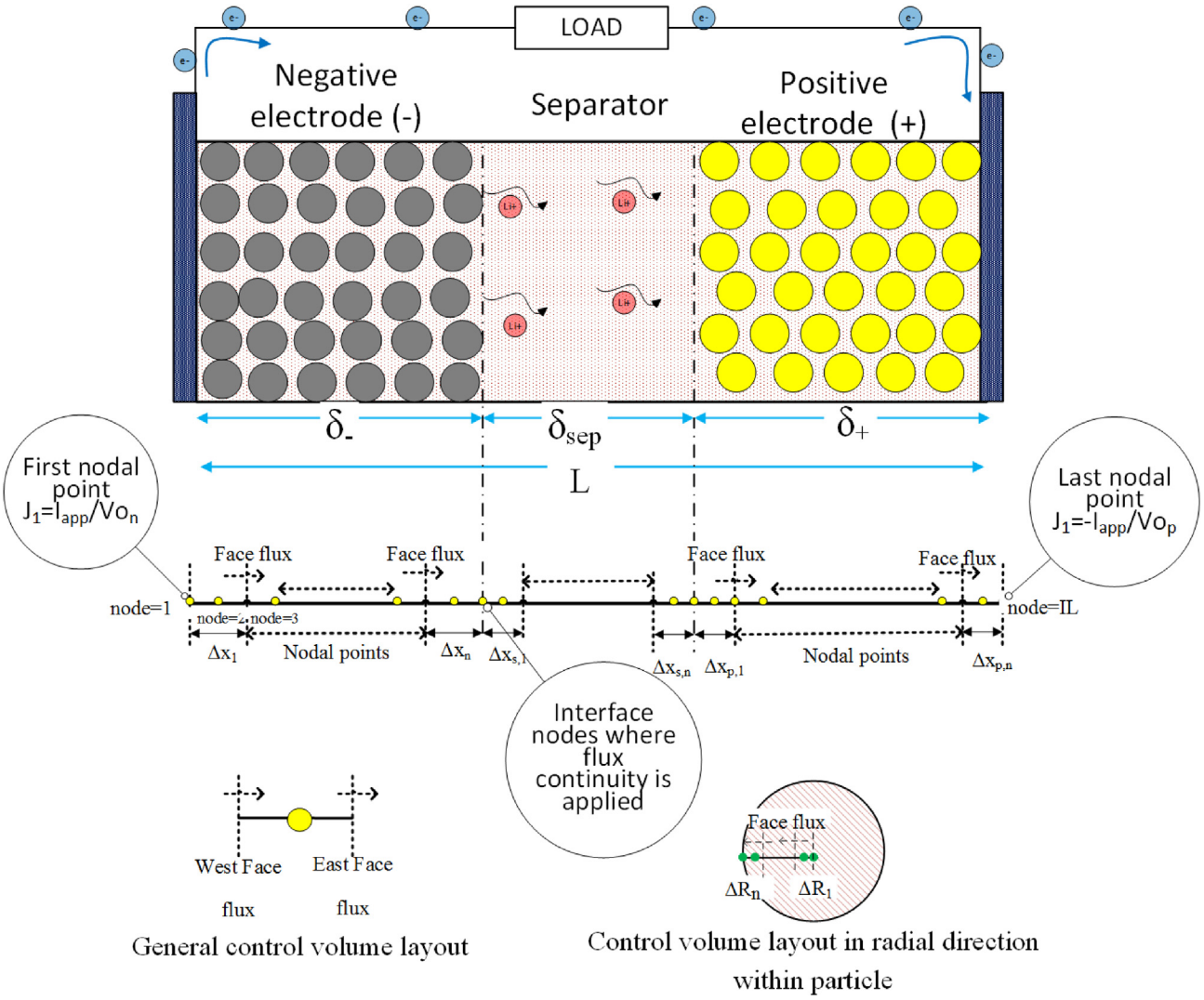

Fig. 1. Battery geometry and finite volume grid layout.

where the Butler-Volmer equation reduces to a quadratic equation and the above equation can be rearranged as:

$$\theta^2 - C\theta - 1 = 0$$

where $C = J_1/a_s i_o$ and i_o is calculated as:

$$i_o = k_{ct}\left(c_s^{max} - c_s^{sur}\right)^{\alpha_n} c_s^{\alpha_p} c_e^{\alpha_n}$$

where at the first and last nodal point in the anode and cathode, the current density is proportional to the externally applied current density. Thus:

$$C = \frac{I_{app}}{A_{n,p} L_{n,p} a_s i_o}$$

The negative part of the solution is neglected and the feasible solution is given by:

$$\theta = \frac{C + \sqrt{C^2 + 4}}{2}$$

The above equation can be rearranged as:

$$\phi_s - \phi_e - U = \frac{RT}{F\alpha_{n,p}} \ln\left(\frac{C + \sqrt{C^2 + 4}}{2}\right)$$

The required solid potential at the first and last nodal point of the battery is given by:

$$\phi_{s,n,1} = \phi_{e,n,1} + U_n + \frac{RT}{F\alpha_n} \ln\left(\frac{C_n + \sqrt{C_n^2 + 4}}{2}\right) \quad (6)$$

$$\phi_{s,p,IL} = \phi_{e,p,IL} + U_p + \frac{RT}{F\alpha_p} \ln\left(\frac{C_p + \sqrt{C_p^2 + 4}}{2}\right) \quad (7)$$

where C_n and C_p represents the constant calculated at the negative and positive electrode respectively.

The above solid potential can be used to correct the solid potential profile obtained by implicitly solving the Poisson's form of the solid potential (Equation (4)). Also the negative open circuit voltage U_n is common for all batteries with a graphite anode. The

re-parametrisation of a battery can be done using the same formulation for the positive OCV as follows.

The cell voltage is calculated as the difference in solid potential at the first and last control volumes $\phi_{s,p,IL} - \phi_{s,n,1}$. In this formulation, the difference of Equation (7) and Equation (6) gives the cell voltage. Thus the required value of $\phi_{s,p,IL}$ can be recalculated from the experimental discharge curve.

$$\phi_{s,p,IL} = V_{cell,measured} + \phi_{s,n,1}$$

Thus in the above equation, the required value of positive OCV to simulate the discharge characteristics is given by:

$$U_p = V_{cell,measured} + U_n + \frac{RT}{F\alpha_n}\ln\left(\frac{C_n + \sqrt{C_n^2+4}}{2}\right) - \phi_{e,p,IL} \qquad (8)$$

$$-\frac{RT}{F\alpha_p}\ln\left(\frac{C_p + \sqrt{C_p^2+4}}{2}\right)$$

As mentioned already, the electrolyte potential at the first node $\phi_{e,n,1}$ is taken as zero in this formulation to fix the solution of electrolyte potential. The measured voltage $V_{cell,measured}$ can be of any C-rate. The cell chemistry is absorbed into the U_p profile through the discharge curve.

2.6. Solvent reduction reaction

The capacity fading solvent reduction side reaction:

$$J_s = -a_n i_{os} e^{(-\alpha_c f \eta_s)} \qquad (9)$$

The modification and the assumptions applied to the over potential, can be seen in Ashwin et al. [8]. The total current density at the first nodal point with the ageing model can be recalculated as:

$$J = \frac{I_{app}}{A_n L_n} = J_1 + J_s \qquad (10)$$

With ageing reaction included, the constant for framing the quadratic form of Butler-Volmer is given by:

$$C = \frac{J_1}{i_o a_s}$$

The calculations involving the solvent reaction side reaction need to be handled iteratively to find the solid potential at first nodal point. This is because the negative current density is non-linearly coupled to the over potential. In the present model, the current density is found to be converging within ten iterations.

2.7. Equation for variable porosity

$$\frac{\partial \varepsilon_e}{\partial t} = a_s(J_1 V_{Li^+} + J_s V_{Lac}) \qquad (11)$$

where V_{Li^+} is the partial molar concentration for intercalation reaction and V_{Lac} is the partial molar concentration for solvent reduction side reaction. The reversible porosity change gets accelerated by increasing the partial molar concentration of the intercalation reaction V_{Li} while the irreversible filling due to SEI gets accelerated by increasing the partial molar concentration for the side reaction V_{Lac}.

2.8. Temperature dependency of properties

Change in temperature will affect the physiochemical property Ψ according to:

$$\Psi = \Psi_{ref}\exp\left[\frac{E_{act}^{\Psi}}{R}\left(\frac{1}{T_{ref}} - \frac{1}{T}\right)\right]$$

The reference temperature is $T_{ref} = 298.15$ K and the activation energy (E_{act}) for each parameter is listed in Table 1 and must be further parametrised against voltage measured at high temperature. However the values listed in Table 1 hold good upto 35 °C.

3. Solution method and flow chart

The equations are solved in a sequential way starting with solving the Lithium in electrolyte phase and the Lithium in solid phase. The electrolyte and solid potential profile can be calculated by solving the Poisson's form of equation. The quadratic form of the Bulter-Volmer equation is solved to find the required solid potential at the first and last nodal points and the solid potential profile is corrected to the required value from Equation (6) and Equation (7). The solution algorithm is explained in Fig. 2a. Inner iterations are provided to enhance coupling between equations. The equations are under-relaxed to handle current variation while applying a dynamic drive cycle. More details of the numerical method can be found in Ref. [18] and an application of the method in Ashwin et al. [19] The discretisation of equations form a tri-diagonal form of matrix which is solved using Tri Diagonal Matrix Algorithm (TDMA).

The above algorithm can be used to calculate the positive electrode open circuit potential to re-parametrise the battery. A detailed flow chart is presented in Fig. 2b. The unknown electrochemical values are taken from different battery modelling literature for re-parametrisation whereas the measured values are accepted without any change. The uncertainty in measurement is the motivation for taking values from different literature which can cause large error in the conventional P2D modelling with measured U_p profile. The model is started with an assumed or known positive open circuit voltage, in this work the U_p profile is from Smith and Wang [13]. The first observable impact of introducing different electrochemical parameters from different studies, on the performance of the battery, is the change in discharge time, the deviation from stoichiometric limits and the variation in the battery voltage. The stoichiometric limits and the running time of the battery can be corrected by adjusting the particle radius (Λ) and the solid diffusion (D_s) coefficient. Adjustments in the side reaction exchange current density (i_{os}) and the partial molar concentration (V_{Li^+},V_{Lac}) is needed only if the ageing and variable porosity equations are solved. A detailed sensitivity study is presented in Section 4 which show the battery operating time and stoichiometric limit is within the required range. The optimised set of electrochemical values are used to calculate the required positive open circuit voltage using Equation (8) for a 1C discharge condition. Now the calculated U_p will update the voltage limit of the battery within the required limit. The U_p calculation is repeated for several iterations to bring down the RMSE below the required limit. This is due to the fact that $\phi_{e,p,IL}$ need few iterations to converge. The OCV for positive

Table 1
Activation energies for the Arrhenius correction [13].

	Negative electrode	Separator	Positive electrode
Exchange current densities, $E^{i_{0-}}$, $E^{i_{0+}}$	3×10^4		3×10^4
Solid phase diffusion coefficient, $E^{Ds_-}_{act}$, $E^{Ds_+}_{act}$	4×10^4		2×10^4
Electrolyte phase diffusion coefficient, E^{De}_{act}	1×10^4	1×10^4	1×10^4
Electrolyte phase conductivity, E^{κ}_{act}	2×10^4	2×10^4	2×10^4

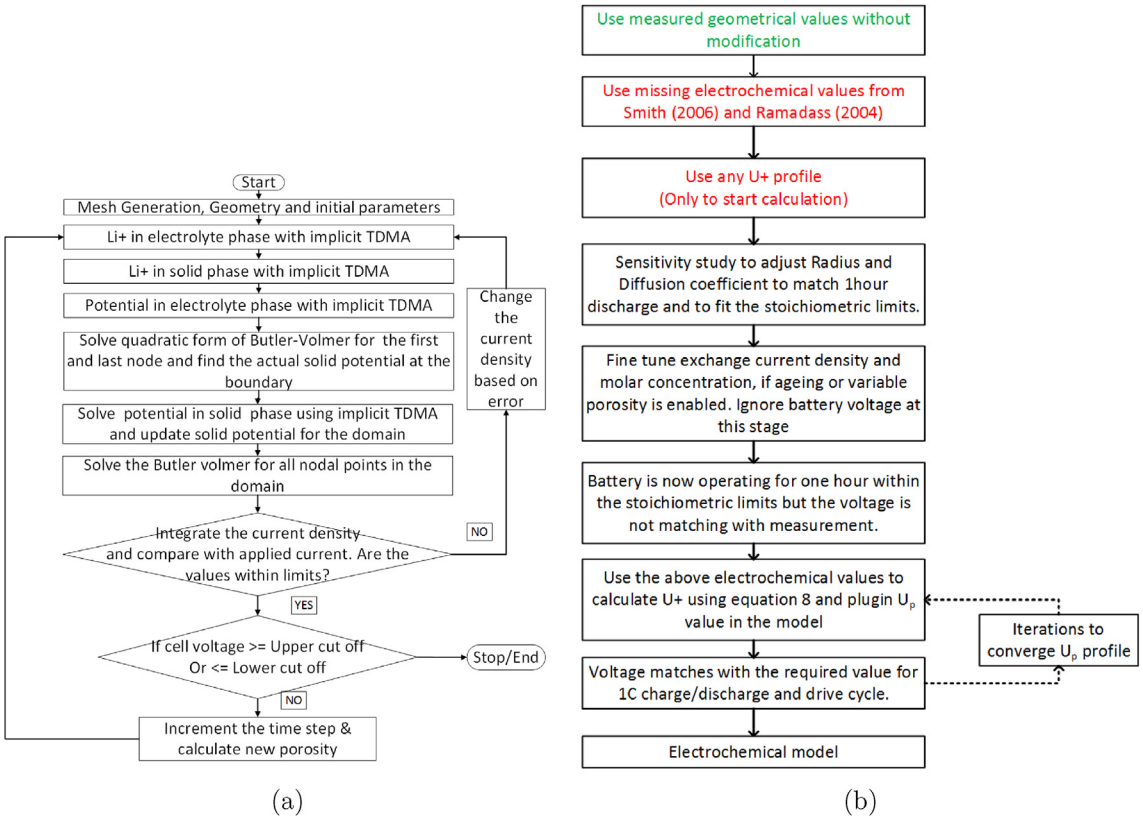

Fig. 2. Algorithm for FORTRAN code and flow chart for re-parameterisation. (a)Algorithm for single cell calculation. (b)Flow chart for re-parametrisation model.

electrode can be fitted into the following expression.

$$U_p = A1 \times e^{-\left[\frac{\chi - B1}{C1}\right]^2} + A2 \times e^{-\left[\frac{\chi - B2}{C2}\right]^2} + A3 \times e^{-\left[\frac{\chi - B3}{C3}\right]^2} + A4 \times e^{-\left[\frac{\chi - B4}{C4}\right]^2} + A5 \times e^{\left[-\frac{\chi - B5}{C5}\right]^2} + A6 \times e^{-\left[\frac{\chi - B6}{C6}\right]^2} + A7 \times e^{-\left[\frac{\chi - B7}{C7}\right]^2} + A8 \times e^{-\left[\frac{\chi - B8}{C8}\right]^2} \quad (12)$$

4. Sensitivity analysis of electro-chemical parameters

The electro-chemical parameters for the battery can be obtained from the technical information provided by the manufacturer or from similar literature. In this study, most of the electro-chemical parameters are taken from the study by Smith and Wang [13] and Ramadass et al. [2] for a SONY18650 battery. The existing electro-chemical values need to be further fine tuned to re-parametrise the model for a NCR18650BD with a different cell chemistry. The cell geometrical parameters are measured in the laboratory and accepted without modification. Also the porosity values are summed to unity in both electrodes. The most critical electro-chemical parameters are found to be the particle radius, diffusion coefficient, partial molar concentration and the exchange current density for ageing reaction. The particle radius and diffusion coefficient influences the stoichiometric ratio and discharge time of the battery. Partial molar concentration affects the porous filling and the side reaction exchange current density affects the capacity fading of the battery. A detailed analysis for fine-tuning these parameters within the operating limit is presented in this section.

Fig. 3a shows that decreasing the particle radius in the positive electrode increases the operating time of the battery. The radius of the particle must be further fine tuned to obtain the correct stoichiometry. A smaller particle radius causes an increase in the volume specific area of the particle a_s. This has two major effects on the battery chemical reaction. The current density for intercalation reaction J_1 can increase whereas the radial gradient at the surface of solid particle $\partial c_s/\partial r$ decreases. The radial gradient has more pronounced effect in controlling the stoichiometry of the system than

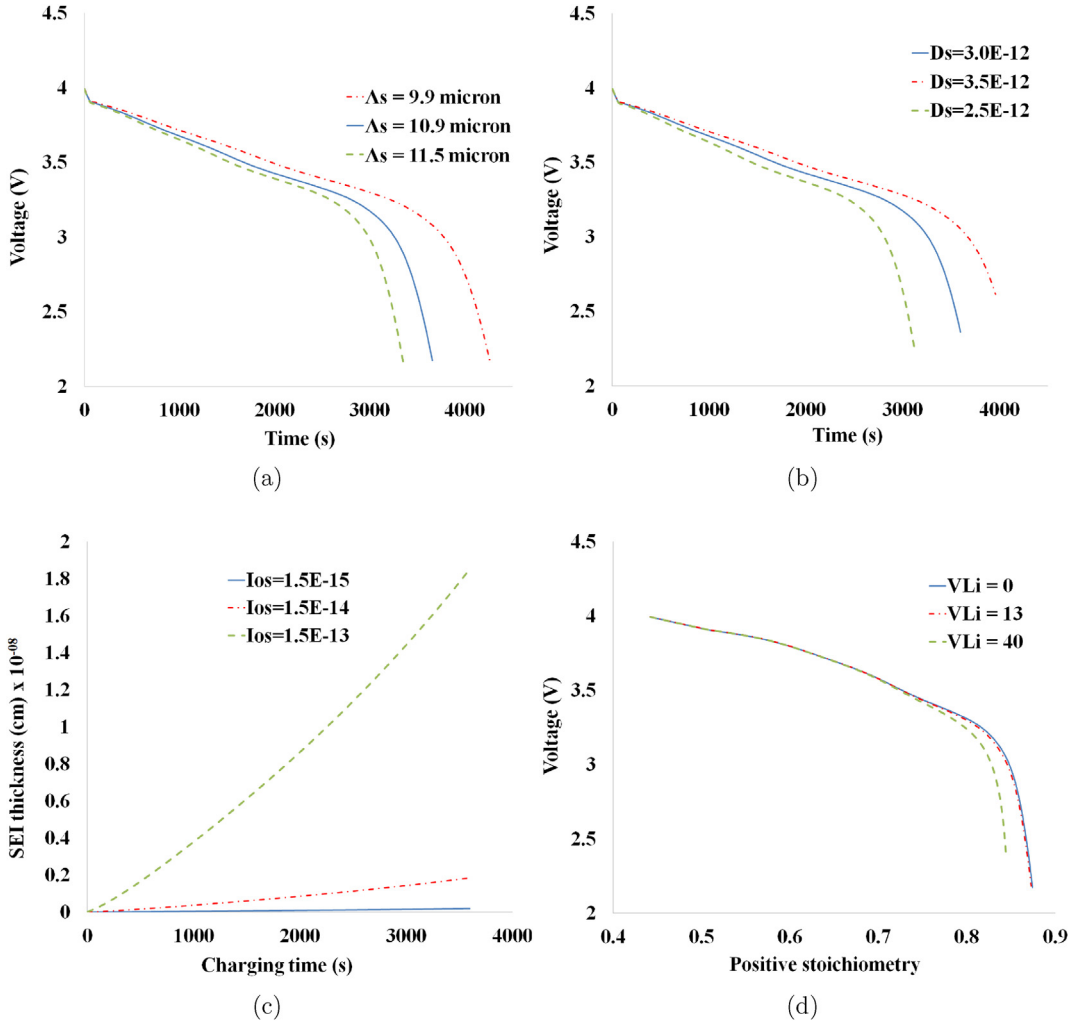

Fig. 3. Sensitivity analysis of different electro-chemical parameters (a)Discharge profile with different particle size. (b) Discharge profile with different diffusion coefficient. (c) SEI growth with different exchange current density. (d) Positive electrode stoichiometry with different partial molar concentration.

the current density and therefore the overall rate of change of stoichiometry decreases. Thus a decrease in the particle radius decelerates the rate of deposition of solid lithium on the surface of the solid particle.

The solid diffusion coefficient together with the particle radius can influence the stoichiometry of the battery. The details can be found in Fig. 3b. Hence both parameters must be simultaneously adjusted to achieve the required performance. The sensitivity of the negative OCV can be further decreased by increasing the stoichiometry of the negative electrode for 0% SOC. This reduces the range of OCV variation in the negative electrode. The modification of the positive OCV is enough to bring down the error to an acceptable limit.

Another important parameter is the exchange current density for solvent reduction side reaction (i_{os}). Fig. 3c shows the SEI thickness with different exchange current densities. Fig. 3d shows the effect of partial molar concentration over the positive electrode stoichiometry. The run with zero partial molar concentration results in no porosity change and hence the available area for reaction remains constant (a_s). Whereas the run with high V_{Li} results in an increase in solid porosity (ε_s) resulting in an increased volume specific reacting area a_s.

The motivation for the above sensitivity study is the difficulty in measuring the P2D model parameters accurately. Applying the modified U_p in the P2D model will correct the operating voltage of the battery to the required value as follows:

5. Experimental validation of the model

The re-parametrisation of the P2D model for a NCR18650BD battery is completed by modifying the OCV for the positive electrode. A detailed algorithm for U_p calculation is presented in Fig. 2b, and this algorithm is again based on calculations from Equation (8). The modified U_p, helps the battery to attain the required operating voltage within 0% SOC and 100%SOC limits. Fig. 4a show plot of modified OCV within the stoichiometric limits. A correlation is then fitted to this plot and it can be found in Equation (12). It is worth noting that the correlation 12 is based on the set of electrochemical values presented in Table 2. A different set of electrochemical values may result in a different U_p correlation. This model does not use the measured value of OCV for any calculation instead it uses the calculated U_p from correlation.

The simulated model is compared with 1C discharge curve as shown in Fig. 4b. The voltage of the battery is recorded at 60 s intervals for 1C measurement. The RMSE for the model compared to the measurement is found to be less than 3.4 mV. This figure only

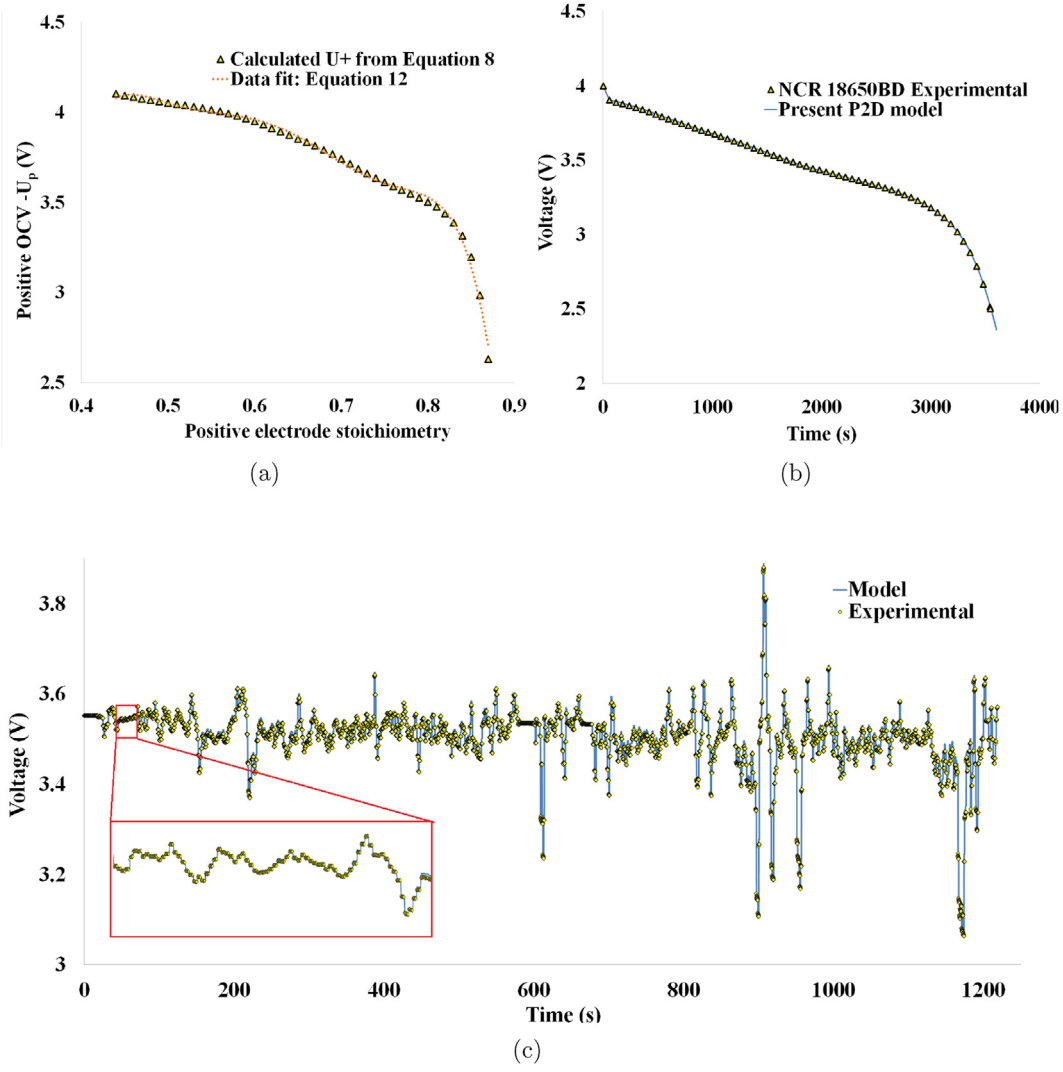

Fig. 4. Electrochemical model predictions of NCR18650BD with modified parameters (a) Calculated positive electrode OCV of NCR18650. (b) Discharge characteristics of NCR18650BD at 25 °C. (c) Drive cycle validation of NCR18650 model at 35 °C.

gives a qualitative indication about model behaviour since the 1C discharge curve is used for the calculation of U_p profile. Therefore a more dynamic drive cycle validation is done to test the model behaviour as follows:

Fig. 4c shows the validation of the present model with a dynamic drive-cycle voltage profile recorded from a prototype electric vehicle when driving in an urban environment with frequent accelerations and regenerative braking events. The battery is started with 35% SoC at a constant temperature of 35 °C. Thus including some temperature dependency of the validation compared to the parameterisation. The peak current variation is 9.93 A while discharging and 10.4 A while charging. This aggressive current pulse takes the battery from 0.01C to 3.5C within a short time step of 1 s. The model is found to agree with the measured values within root mean square error (RMSE) of 8.9 mV and peak error (PK Error) of 26.0 mV. A comparison of the RMSE and PK Error of the present model with the literature results of the widely accepted SONY Li_yCoO_2 model are presented in Table 3. It can be seen that the error of the current model is lower than that of the SONY battery model for 1C discharge.

6. Conclusion

An implicit finite volume-finite difference formulation is used to re-parametrise the P2D model for any cell chemistry with known cathode OCV. The uncertainty in determining exact electrochemical values can be handled in this formulation by modifying the anode OCV. This method, considered as the best to re-parametrise a P2D model for any cell chemistry, has been implemented in this paper for the first time. A numerical expression is derived to calculate anode OCV based on a simplified quadratic equation for Bulter-Volmer kinetics. Inclusion of this equation in the model is found to reduce the computation time drastically compared to iterative methods. The experimental result needed to re-parametrise the battery, reduces to the measurement of discharge voltage. The computational model is applied to re-parametrise NCR18650BD battery. A sensitivity study is performed in the electrochemical parameters. The model is validated against the full drive cycle and the RMSE and Peak errors are found well within the acceptable limit. The model retains the numerical accuracy whilst comparing with the models presented in the literature. This work proves that the electro-chemical model can be easily parametrised for an any chemistry.

Table 2
Optimised electrochemical parameters for NCR18650BD battery.

	Negative electrode	Separator	Positive electrode
Thickness, δ	149.9×10^{-4}	20.0×10^{-4}	134.0×10^{-4}
Particle radius, Λ_s	10.9×10^{-4}		10.9×10^{-4}
Active material volume fraction ε_s	0.595	0.0	0.63
Electrolyte phase volume fraction ε_e	0.3	0.5	0.30
Filler material volume fraction	0.105	0.5	0.07
Maximum solid phase concentration $c_{s,max}$	30.6×10^{-3}		51.6×10^{-3}
Stoichiometry at 0% SOC	0.126		0.870
Stoichiometry at 100% SOC	0.676		0.442
Average electrolyte concentration c_e	1.2×10^{-3}	1.2×10^{-3}	1.2×10^{-3}
Exchange current density (i_o)	3.6×10^{-4}		2.6×10^{-4}
Charge-transfer coefficients α_a, α_c	0.5, 0.5		0.5, 0.5
SEI layer film resistance, Ω_{SEI} [a]	10		0.0
Solid phase Li diffusion coefficient D_s	2.7×10^{-12}		3.0×10^{-12}
Solid phase conductivity, σ	1.0		1.0
Electrolyte phase Li^+ diffusion coefficient, D_e	2.6×10^{-6}	2.6×10^{-6}	2.6×10^{-6}
Bruggeman porosity exponent, p	1.5	1.5	1.5
Electrolyte activity coefficient, $f^{\pm}$	1.0	1.0	1.0
Li^+ transference number t_+^0	0.363	0.363	0.363
Reference voltage U_{ref} [a]	0		0
Molecular weight M_p	7.3×10^4		
Density of SEI Layer ρ_p	2.1×10^{-3}		
Side reaction exchange current density i_{os} [a]	1.5×10^{-12}		
Conductivity of SEI Layer κ_p [a]	1×10^{-4}		

[a] Assumed values.

Table 3
Error comparison of different models for 1C discharge and the drive cycle at 30% SoC and 35°C.

	RMSE (mV)	PK Error (mV)	Calculation time (s)
Electro-chemical model NCR18650BD	2.20	3.01	38
Electro-chemical model Li_yCoO_2 [a]	3.04	4.02	56
Electro-chemical model NCR18650BD [b]	8.9	26.0	

[a] Ashwin et al. [8].
[b] Full drive cycle validation.

Acknowledgement

This work was funded by Innovate UK through the WMG centre High Value Manufacturing (HVM) Catapult in collaboration with Jaguar Land Rover and TATA Motors European Technical Centre.

Nomenclature

a	active surface area per electrode unit volume ($3\varepsilon/\Lambda$) (cm^{-1})
A	Electrode plate area (cm^2)
c	Volume-averaged concentration (mol cm^{-3})
D	Diffusion coefficient (cm^2 s^{-1})
i_o	Exchange current density for intercalation reaction (A cm^{-2})
i_{os}	Exchange current density for solvent reduction reaction (A cm^{-2})
I_{app}	Applied current (A)
J_1	Reaction current for intercalation reaction (A cm^{-3})
J_s	Reaction current for solvent reduction reaction (A cm^{-3})
k_{ct}	Kinetic rate constant for intercalation reaction
L	Cell width (cm)
r	Radial coordinate (cm)
t	Time (s)
U	Open Circuit Voltage, OCV (V)
V	Cell voltage (V)
$V_{cell,measured}$	Measured terminal voltage (V)
V	Partial molar volume (cm^3 mol^{-1})

Greek symbols

α	Charge-transfer coefficient
ε	Volume fraction of domain
Λ	Particle radius (cm)
κ	Conductivity of electrolyte (S cm^{-1})
κ_D	Diffusivity (A cm^{-1})
χ	Stoichiometric ratios in the electrode
σ	Solid phase conductivity (S cm^{-1})
ϕ	Volume averaged potential (V)

Superscript & subscript

1	First Cartesian or Radial control volume
IL	Last Cartesian control volume
rl	Last Radial control volume
e	Electrolyte phase
eff	Effective
max	Maximum
n, *p*	Negative and positive electrode
s	Solid phase
sur	Surface quantity

References

[1] M. Doyle, T.F. Fuller, J. Newman, J. Electrochem. Soc. 140 (1993) 1526–1533.
[2] P. Ramadass, B. Haran, P.M. Gomadam, R. White, B.N. Popov, J. Electrochem. Soc. 151 (2004) A196–A203.
[3] J. Groot, M. Swierczynski, A.I. Stan, S.K. Kær, J. Power Sources 286 (2015) 475–487.
[4] L. Cai, R.E. White, J. Power Sources 196 (2011) 5985–5989.
[5] M. Guo, R.E. White, J. Power Sources 221 (2013) 334–344.

[6] Y. Xie, J. Li, C. Yuan, J. Power Sources 248 (2014) 172–179.
[7] T.R. Tanim, C.D. Rahn, J. Power Sources 294 (2015) 239–247.
[8] T. Ashwin, Y.M. Chung, J. Wang, J. Power Sources 328 (2016) 586–598.
[9] C. Wang, W. Gu, B. Liaw, J. Electrochem. Soc. 145 (1998) 3407–3417.
[10] V.R. Subramanian, J.A. Ritter, R.E. White, J. Electrochem. Soc. 148 (2001) E444–E449.
[11] B.S. Haran, B.N. Popov, R.E. White, J. Power Sources 75 (1998) 56–63.
[12] S. Santhanagopalan, Q. Guo, P. Ramadass, R.E. White, J. Power Sources 156 (2006) 620–628.
[13] K. Smith, C.-Y. Wang, J. Power Sources 160 (2006) 662–673.
[14] B. Wu, V. Yufit, M. Marinescu, G.J. Offer, R.F. Martinez-Botas, N.P. Brandon, J. Power Sources 243 (2013) 544–554.
[15] T.-S. Dao, C.P. Vyasarayani, J. McPhee, J. Power Sources 198 (2012) 329–337.
[16] J.L. Lee, A. Chemistruck, G.L. Plett, J. Power Sources 220 (2012) 430–448.
[17] S. Santhanagopalan, Q. Guo, R.E. White, J. Electrochem. Soc. 154 (2007) A198–A206.
[18] S. Patankar, Numerical Heat Transfer and Fluid Flow, CRC Press, 1980.
[19] T. Ashwin, G. Narasimham, S. Jacob, Int. J. Heat Mass Transf. 54 (2011) 3357–3368.